Dynamic Roughening of Tetrahedral Amorphous Carbon

C. Casiraghi,[1,*] A. C. Ferrari,[1] R Ohr,[2] A. J. Flewitt,[1] D. P. Chu,[3,1] and J. Robertson[1]
[1]*Engineering Department, Cambridge University, Cambridge CB2 1PZ, United Kingdom*
[2]*IBM STD, Hechtsheimerstrasse 2, D-55131 Mainz, Germany*
[3]*Cambridge Research Laboratory of Epson, 9a Science Park, Cambridge CB4 0FE, United Kingdom*
(Received 25 July 2003; published 25 November 2003)

The roughness of tetrahedral amorphous carbon (ta-C) films grown at room temperature is measured as a function of film thickness by atomic force microscopy, to extract roughness and growth exponents of $\alpha \sim 0.39$ and $\beta \sim 0$–0.1, respectively. This extremely small growth exponent shows that some form of surface diffusion and relaxation operates at a homologous temperature of 0.07, much lower than in any other material. This is accounted for by a Monte Carlo simulation, which assumes a smoothening during a thermal spike, following energetic ion deposition. The low roughness allows ta-C to be used as an ultrathin protective coating on magnetic disk storage systems with $\sim$1 Tbit/in.^{2} storage density.

DOI: 10.1103/PhysRevLett.91.226104 PACS numbers: 68.35.Ct, 68.55.–a, 81.15.–z, 85.70.Li

The evolution of the surface roughness of growing thin films of metals or semiconductors provides much information about their growth mechanism. Some systems show stages of nucleation, coalescence, and growth. Some systems show microstructures that vary with the growth temperature and conditions [1]. Others show a self-affine behavior in which the roughness varies in a fractal manner with the film thickness and the measurement scale [2–6]. In this case, the randomness of the incident flux creates roughness, which is smoothed by the presence of surface diffusion or surface relaxation and a minimization of surface energy. It is found that the roughness evolution belongs to certain classes depending on the dominant process. These processes are thermally activated, so the observed behavior class depends on the temperature scaled to the melting point—homologous temperature, θ—for a given class of materials.

This Letter presents the first measurement of the roughness evolution of a highly sp^3 form of amorphous diamondlike carbon called tetrahedral amorphous carbon (ta-C) grown from energetic ions [7]. It is found to have an extremely small roughness, of $\sim$0.1 nm root mean square (rms), and an extremely small growth exponent, and to have these at very low homologous temperatures, of order 0.07, based on a melting point of 4000 K [8]. These results indicate that surface relaxation is occurring at very low scaled temperatures. We interpret this as a smoothening that occurs during a local surface melting caused by the incident ions. This is very important technologically, as the remarkable smoothness of ta-C allows it to form pinhole-free films of only 1–2 nm thickness, and to act as a protective layer on read heads and disks in magnetic disk storage systems [9]. While the traditional carbon coatings for magnetic storage cease to protect below 3–4 nm [10], 1–2 nm thick ta-C films could be used to achieve recording densities over $\sim$100 Gbit/in.^{2} and $\sim$1 Tbit/in.^{2} for longitudinal and vertical recording, respectively [11–13].

The ta-C films are deposited on two different filtered cathodic vacuum arc (FCVA) systems, one a lab-scale integrated off-plane double bend (S-bend) [14], the other a high current arc (HCA) in a production near process environment [15]. In the first case, the deposition rate is 0.8 nm/s and the film thickness is between 4 and 70 nm, as derived from a combination of deposition rate measurements, ellipsometry, and x-ray reflectivity (XRR). The ta-C films are deposited on silicon (100) substrates previously cleaned with acetone in an ultrasonic bath. This gives a substrate rms roughness of $\sim$0.2 nm. For HCA films, the deposition rate is 8–10 nm/s and the film thickness is between 1 and 20 nm as determined by x-ray reflectivity and ellipsometry. These films were deposited on ultrasmooth silicon with rms roughness $\sim$0.1 nm. The thickness determination by XRR is precise to 0.1 nm [12]. The atomic force microscope (AFM) noise is less than 0.05 nm in the vertical dimension. Both sets of films were deposited at a base pressure of $\sim 10^{-4}$ Pa, at room temperature and with no substrate bias. The self-bias results in an ion energy of about 20–40 eV [7,15].

The surface morphology is measured by a Nanoscope III, Digital Instrument AFM operated in air and in tapping mode. The AFM tips are etched silicon with a resonant frequency of 254–390 kHz and a cantilever length of 160 μm. A surface size of 1 μm $\times$ 1 μm is scanned. The rms roughness (R) was calculated on a 0.5 μm $\times$ 0.5 μm area to avoid any macroparticles [14]. The roughness R is defined as

$$R = \left[\sum (h_i - h_{\text{ave}})^2/\text{N}\right]^{1/2}, \quad (1)$$

where h_i is the film height, h_{ave} is the average of the height values in a given area, and N is the number of points. Each image consists of 254 line scans. The R values were computed after image "flattening." This procedure is standard on commercial instruments to account for the

fact that virtually all samples are macroscopically tilted with respect to the horizontal scan directions of the microscope. This procedure could affect only the components of the surface roughness with characteristic wavelength significantly exceeding the scan size (> 1 μm in our case) [16].

The roughness is assumed to follow a self-affine behavior [17–21], in which R scales as

$$R \sim \ell^{\alpha} f(t/\ell^{\alpha/\beta}), \tag{2}$$

where t is the deposition time with deposition rate assumed constant and ℓ is the length scale, i.e., $\ell \times \ell$ is the window size where R is measured, with $\ell \leq L$, size of the sample. $f(u)$ is the scaling function of the argument $u = t/\ell^{\alpha/\beta}$. For small times, $u \ll 1$, then $R \sim t^{\beta}$ and the different surface sites are independent. As time increases, different sites become correlated. When the correlations are significant, the roughness saturates at a constant value R_{sat}. α is the roughness exponent ($0 \leq \alpha \leq 1$). β is the growth exponent. For a constant deposition rate, β is found by plotting R against thickness z for a series of samples grown for increasing deposition times. The two sets of films examined in this paper were grown with two fixed deposition rates. Thus, from (2) their roughness scales as $R \sim z^{\beta}$, regardless of the deposition rate used to grow each set of films.

The exponents α and β uniquely characterize how a surface evolves with length scale ℓ and time t. Their values define the growth mechanism [20]. For random deposition, the particles stick at the surface, giving $\beta = 0.5$ and α is undefined. For random deposition with surface diffusion, the particles do not stick irreversibly, but can relax to a nearby site of lower height. This model gives $\beta = 1/3$ and $\alpha = 1$. The ballistic deposition is different from the random deposition because lateral sticking is allowed. This gives $\beta = 0.5$ and $\alpha = 2/3$.

The scaling exponents α and β can also be measured by studying the height-height correlation function $H(r, t) = \langle [h(r, t) - h(0, t)]^2 \rangle$, where r is the lateral surface position and $h(r, t)$ is the surface height at position r and deposition time t. The brackets denote spatial average. For self-affine structures, $H(r, t)$ behaves asymptotically as [20]

$$H(r, t) \sim r^{2\alpha} \qquad \text{for } r \ll \xi, \tag{3}$$

$$H(r, t) \sim 2R_{\text{sat}}^2 \qquad \text{for } r \gg \xi. \tag{4}$$

ξ is the correlation length, defined as the largest distance at which the height is still correlated. $H(r, t)$ can be used to give an independent value of roughness exponent α for each film. As [20]

$$\xi(t) \sim t^{\beta/\alpha}, \tag{5}$$

β is then derived by plotting ξ versus thickness on a log-log plot.

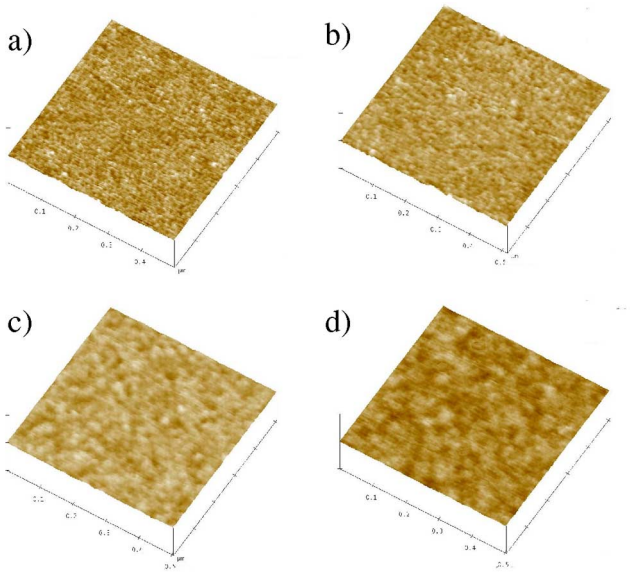

FIG. 1 (color online). AFM image of ta-C films with thickness (a) 1.6 nm deposited by HCA, (b) 3 nm by HCA, and 15 m (c) and 60 nm (d) by FCVA. The vertical scale is 10 nm.

Figure 1 shows surface images of ta-C films of thickness (a) 1.6 nm, (b) 3 nm, (c) 15 nm, and (d) 55 nm. The surface is continuous over a large area and is characterized by uniformly distributed features.

Figure 2 shows the roughness evolution as a function of film thickness. The roughness of ta-C films stays almost constant, from 0.12 nm at 0.9 nm thickness to 0.11 nm at 60 nm thickness. The roughness is very low and is similar to previous data on thicker films [22,23]. It is lower than that of sputtered a-C:H [24] and a-C:N [25]. For the lab-scale FCVA films, the roughness decreases initially as the films cover the underlying rougher Si substrate used in that case. The Si substrates for the production near process HCA films are much smoother. Otherwise, both sets of films would show essentially a similar, constant roughness over the range of film thickness studied. Thus, both data sets give a growth exponent $\beta \sim 0$.

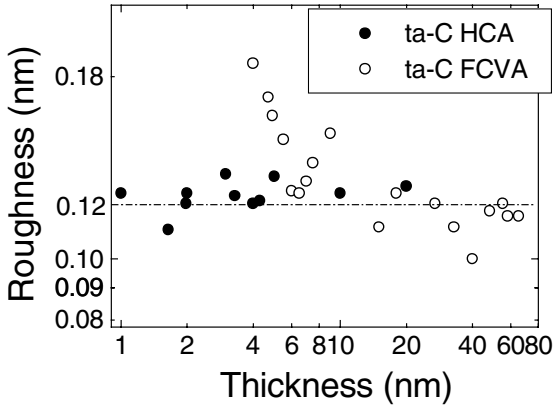

FIG. 2. rms surface roughness as a function of film thickness. The roughness is constant (~ 0.12 nm).

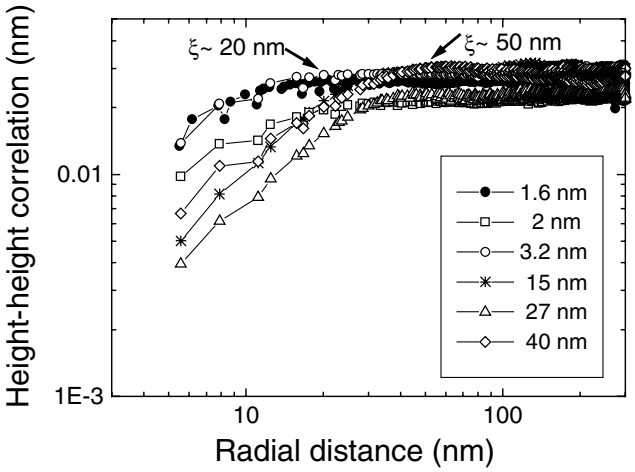

FIG. 3. Height-height correlation function for different thicknesses. The initial slope gives the roughness coefficient α [Eq. (3)], the turning point gives the correlation length [Eq. (4)]. 1.6, 2, and 3.2 nm are HCA films; 15, 27, and 40 nm are FCVA films.

Figure 3 plots $H(r, t)$ for different samples against r. The roughness exponent α is derived from the slope of the curves before saturation. We find α between 0.25 and 0.6 (average value is 0.39). For large r (~ 100 nm), each curve turns into a plateau. From Eq. (4), this saturation value is related to the film roughness for that thickness. The roughness derived from $H(r, t)$ and Eq. (4) is in good agreement with the roughness measured directly by AFM. The inflection point in the curves of Fig. 3 determines the lateral correlation length ξ. By plotting ξ versus time, Eq. (5) gives $\beta/\alpha \sim 0.24$, as shown in Fig. 4. Using our α values, we find β is between 0.06 and 0.12. This is in good agreement with β derived from Fig. 2.

Thus, the scaling exponents for ta-C are $\alpha \sim 0.39$ and $\beta \sim 0$–0.12. These exponents do not match any of the existing growth mechanisms [20] such as the continuum models of Kardar-Parisi-Zhang [19] or Edwards-Wilkinson [18].

It is well known that diamondlike carbon films deposited at room temperature are smooth. The mechanism of this smoothness was not previously defined. The smoothness correlates with high sp^3 bonding [23]. The origin of the sp^3 bonding has been extensively studied. It is attributed to a subplantation process, in which the film grows from energetic ions, which implant themselves just below the surface [26–29]. However, it is not subplantation itself that causes the smoothness.

Growth exponents $\beta \sim 0$ generally arise from surface diffusion and relaxation, as noted by Tamborenea and Das Sarma [30]. We use a simple model to account for the smoothening process. We assume that the energy of the depositing ions dissipates locally as heat in a so-called thermal spike of $\sim$1 ps [31] and that this heat causes a local surface melting. During this time, surface

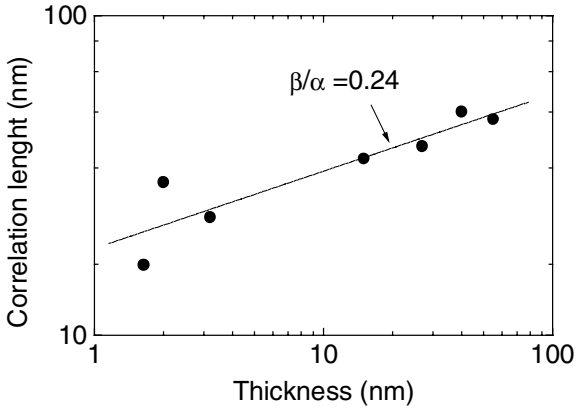

FIG. 4. Plot of the correlation length against the thickness. The slope of the line gives β/α [Eq. (5)].

energy minimization flattens the surface locally. Figure 5 shows a schematic representation of the surface before and after the local melting effect.

We model this by a Monte Carlo simulation. The only free parameter is the number of nearest neighbors in the melted zone. We consider up to three nearest neighbors to be affected. We simulated films of increasing thickness up to 30 monolayers, and with a cell size of 512×512 atoms. Figure 6 shows an example of the resulting surface. The growth exponent β depends little on number of neighbors, varying from 0.08 (first neighbors) to 0.15 (third neighbors). The roughness exponent α increases slowly with number of neighbors from 0.26 (first neighbors) to 0.36 (third neighbors). Thus, the growth exponents derived from our simulations well agree with the experimental data.

The remarkable fact of ta-C is that this surface relaxation process should occur at room temperature, which is a homologous temperature $\theta \sim 0.07$ [8]. Diffusion and relaxation (creep) are both thermally activated processes, whose activation energy is proportional to the bond energy and thus melting temperature. Hence, surface diffusion sets in typically at $\theta \sim 0.4$ on Thornton diagrams [1]. Clearly, the energetic ions involved in ta-C

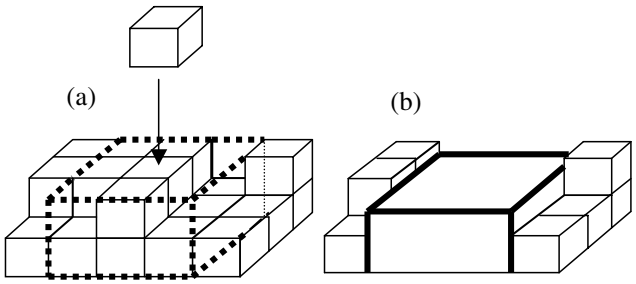

FIG. 5. Model used in the Monte Carlo simulation. (a) The energy of an incident ion dissipates in a thermal spike volume (dotted line). (b) This causes local melting and flattens the surface locally.

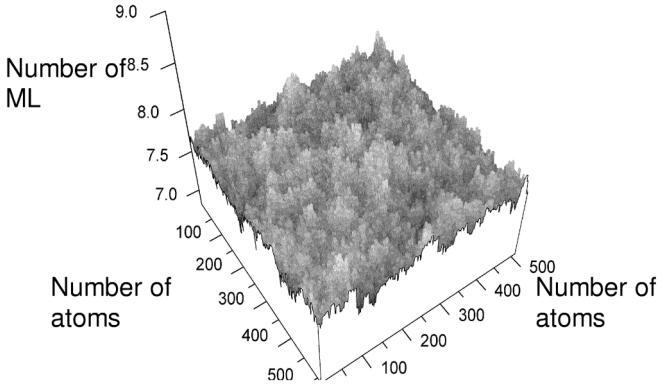

FIG. 6. Simulated surface after thermal spikes cause a flattening to second neighbors of the incident ion. The scaling exponents are $\beta \sim 0.1$ and $\alpha \sim 0.32$.

deposition and, to a lesser extent, other diamondlike carbons allow relaxation at much lower homologous temperatures.

The final question involves the temperature dependence of roughness. It was reported that the roughness of ta-C suddenly increases when it is deposited above a critical temperature of ~150–250 °C [23,32]. This apparently contradicts our model. This is resolved by noting that the outer atomic layer reconstructs as a graphite layer lying in the plane of the surface [33]. This allows local melting to flatten the surface. However, above the critical temperature, the bulk bonding reverts to sp^2, and the graphitic planes now lie normal to the film surface [28,34]. It is not possible to flatten these surfaces by melting. Finally, our model is also valid for hydrogenated ta-C (ta-C:H). We find that the roughness of ta-C:H is also very low (0.13 nm).

In conclusion, we have reported the first investigation of the kinetic surface evolution of ta-C surface and its fractal analysis. We find that a growth exponent β of 0 to 0.12, a roughness exponent $\alpha \sim 0.39$, and an extremely small roughness of order 0.1 nm. We propose that this low roughness arises from a local melting during energetic ion deposition. This implies that ta-C satisfies the requirements for the ultimate storage density of ~1 Tbit/in.^{2}.

C. C. acknowledges the EU project FAMOUS. A. C. F. acknowledges funding by the Royal Society.

*Electronic address: cc324@eng.cam.ac.uk

[1] J. A. Thornton, J. Vac. Sci. Technol. **11**, 666 (1974).
[2] H. You, R. P. Chiarello, H. K. Kim, K. G. Vandervoort, Phys. Rev. Lett. **70**, 2900 (1993).
[3] H. N. Yang, G. C. Wang, and T. M. Lu, Phys. Rev. Lett. **73**, 2348 (1994).
[4] R. Chiarello, V. Panella, J. Krim, and C. Thompson, Phys. Rev. Lett. **67**, 3408 (1991).
[5] M. A. Cotta, R. A. Hamm, T. W. Staley, S. N. G. Chu, L. R. Harriott, M. B. Panish, and H. Temkin, Phys. Rev. Lett. **70**, 4106 (1993).
[6] A. H. M. Smets, W. M. M. Kessels, and M. C. M. van de Sanden, Appl. Phys. Lett. **82**, 865 (2003).
[7] J. Robertson, Mater. Sci. Eng. **R37**, 129 (2002).
[8] J. E. Field, *The Properties of Natural and Synthetic Diamond* (Academic, New York, 1992).
[9] P. R. Goglia, J. Berkowitz, J. Hoehn, A. Xidis, and L. Stover, Diam. Relat. Mater. **10**, 271 (2001).
[10] E. C. Cutiongco, D. Li, Y. W. Chung, and C. S. Bhatia, IEEE Trans. Magn. **33**, 938 (1997).
[11] D. J. Li, M. U. Guruz, C. S. Bhatia, and Y. Chung, Appl. Phys. Lett. **81**, 1113 (2002).
[12] M. Beghi, A. C. Ferrari, K. B. K. Teo, J. Robertson, C. E. Bottani, A. LiBassi, and B. K. Tanner, Appl. Phys. Lett. **81**, 3804 (2002).
[13] R. W. Wood, IEEE Trans. Magn. **36**, 36 (2000).
[14] K. B. K. Teo, S. E. Rodil, J. T. H. Tsai, A. C. Ferrari, J. Robertson, and W. I. Milne, J. Appl. Phys. **89**, 3706 (2001).
[15] T. Witke, T. Schulke, B. Schultrich, P. Siemonth, and J. Vetter, Surf. Coat. Technol. **126**, 81 (2000).
[16] J. Krim, I. Heyvaert, C. Van Haesendonck, and Y. Bruynseraede, Phys. Rev. Lett. **70**, 57 (1993).
[17] F. Family, J. Phys. A **18**, L75 (1985).
[18] S. F. Edwards and D. R. Wilkinson, Proc. R. Soc. London A **381**, 17 (1982).
[19] M. Kardar, G. Parisi, and Y. Zhang, Phys. Rev. Lett. **56**, 889 (1986).
[20] A. L. Barabasi and H. E. Stanley, *Fractal Concepts in Surface Growth* (Cambridge University Press, Cambridge, England, 1995).
[21] S. Das Sarma and P. Tamborenea, Phys. Rev. Lett. **66**, 325 (1991).
[22] X. Shi, L. Cheah, J. R. Shi, S. Zun, and B. K. Tay, J. Phys. Condens. Matter **11**, 185 (1999).
[23] Y. Lifshitz, G. D. Lempert, and E. Grossman, Phys. Rev. Lett. **72**, 2753 (1994).
[24] R. J. Waltman *et al.*, Tribol. Lett. **12**, 51 (2002).
[25] E. Riedo, J. Chevrier, F. Comin, and H. Brune, Surf. Sci. **477**, 25 (2001).
[26] Y. Lifshitz, S. R. Kasi, and J. W. Rabalais, Phys. Rev. Lett. **62**, 1290 (1989).
[27] J. Robertson, Diam. Relat. Mater. **2**, 984 (1993); **3**, 361 (1994).
[28] C. A. Davis, G. A. J. Amaratunga, and K. M. Knowles, Phys. Rev. Lett. **80**, 3280 (1998).
[29] S. Uhlmann, T. Frauenheim, and Y. Lifshitz, Phys. Rev. Lett. **81**, 641 (1998).
[30] P. I. Tamborenea and S. Das Sarma, Phys. Rev. E **48**, 2575 (1993).
[31] N. Marks, J. Phys. Condens. Matter **14**, 2901 (2002).
[32] S. Sattel, J. Robertson, and H. Ehrhardt, J. Appl. Phys. **82**, 4566 (1997).
[33] P. C. Kelires, J. Non-Cryst. Solids **230**, 597 (1998).
[34] Y. Yin, J. Zou, and D. R. McKenzie, Nucl. Instrum. Methods Phys. Res., Sect. B **119**, 587 (1996).